A REAL-TIME HARMONIC DETECTOR DESIGN TO IMPROVE POWER QUALITY IN POWER SYSTEMS

by

Ahmad Yousef Omishat

Submitted in Partial Fulfillment of the Requirements

for the Degree of

Master of Science

in the

Electrical Engineering

Program

YOUNGSTOWN STATE UNIVERSITY

August, 2017

A Real-Time Harmonic Detector Design to Improve Power Quality in Power Systems

Ahmad Yousef Omishat

I hereby release this thesis to the public. I understand that this thesis will be made available from the OhioLINK ETD Center and the Maag Library Circulation Desk for public access. I also authorize the University or other individuals to make copies of this thesis as needed for scholarly research.

Signature:

Ahmad Y Omishat, Student Date

Approvals:

Dr.FrankX.Li, Thesis Advisor Date

Dr.Jalal Jalali, Committee Member Date

Dr.Eric MacDonald, Committee Member Date

Dr. Salvatore A. Sanders, Dean of Graduate Studies Date

Abstract

Power distortion has been a rising concern in the industrialized society nowadays due to the increasing number of non-linear power electronic devices. Power distortion refers to the existence of unwanted frequency harmonics in power systems, which is dangerous and may cause serious problems such as fires, electromagnetic interfaces, and equipment damage. Therefore, detecting harmonics is a critical part of determining the efficiency and the safety of an electrical system. The objective of thesis was to develop a real-time harmonic detection system that can detect the harmonics in a single-phase AC electrical system by using digital hardware. The proposed harmonic detection system was designed with VHSIC Hardware Description Language (VHDL), which can be implemented on a Field-Programmable Gate Array (FPGA) chip. Fast Fourier Transform (FFT) was utilized to get the values for the 1^{st}, 3^{rd}, 5^{th}, 7^{th}, and 9^{th} harmonics of the signals. In this thesis, two artificial harmonic components were constructed to create two test signals using MATLAB to match real life scenarios. Additionally, one actual electrical signal was recorded for comparison. The three signals were then simulated and analyzed through the proposed system. Signals were also processed using MATLAB to get the theoretical values of the harmonics. The digital hardware simulation results of the proposed real-time harmonic detection system matched the theoretical simulations from MATLAB.

Acknowledgements

First and foremost, I thank God for all his blessings and for giving me the courage to complete this research. I would also like to express my deepest gratitude to my research advisor Dr. Frank X. Li for his excellent guidance, advice and patience. I am extremely grateful for my beautiful parents for their unconditional love, care, and sacrifice, and for educating and preparing me for my future. I would also like to thank my brothers and my sisters for all their support, and encouragement. Special thanks go to my friends who have always been there for me. Finally, my thanks go to all the people who have supported me in completing this research directly or indirectly.

Table of Contents

List of Figures

List of Tables

Abbreviations

FFT	Fast Fourier Transform
CGI	Common Gateway Interface
ADC	Analog-to-Digital Convertor
GUIs	Graphical User Interfaces
THD	Total Demand Distortion
DFT	Discrete Fourier Transform
LCD	Liquid-Crystal Display
FPGA	Field-Programmable Gate Array
VHSIC	Very High Speed Integrated Circuit
VHDL	VHSIC Hardware Description Language
DSP	Digital Signal Processing
SMPS	Switched Mode Power Supplies
TDD	Total Demand Distortion
SNR	Signal to Noise Ratio
PLDs	Programmable Logic Devices
FIR	Finite Impulse Response
NCO	Numerically Controlled Oscillator
TCL	Tool Command Language

Chapter 1 - Introduction

1.1 Power Distortion

Today, in an industrialized society, a progressively critical portion of the generated electrical energy is processed via power electronics for different applications in industrial, commercial, residential, and military environments [1]. In recent decades, there has been a rising concern for power system distortion because of the increasing numbers and power ratings of non-linear power electronic devices. Power system distortion is normally expressed in terms of harmonic components. Harmonic pollution in static power converters is a serious problem. For example, in many residential, commercial, and office buildings, the third harmonic creates high neutral currents that may start fires, even when the fundamental neutral current is within acceptable limits [2].

1.2 Harmonics

Harmonics are undesirable currents and/or voltages that exist at some multiple or fraction of the fundamental frequency, which is normally 60 Hz. Common values are the third harmonic (180 Hz), the fifth harmonic (300 Hz), the seventh harmonic (420 Hz), and so on. In converting ac power to dc power, a converter chops the ac current waveform by allowing it to flow only during a certain segment of a cycle. The ac current waveform can be represented by a distorted sinusoidal waveform that can be separated into its harmonic components using Fourier Transform analysis.

1.3 Motivation

Analyzing the harmonic components in the voltage/current waveforms is an important part of an electrical system. Determining the harmonic distortion is the foundation to choose the right power filter for that system. Analyzing the harmonic distortion in a system is usually a lengthy task; it is also not done in real-time, which makes it harder to analyze the system if it is constantly changing. In this thesis, the idea of real-time harmonic analysis will be presented. In other words, since the harmonic distortion level in a power system is constantly changing due to the changes that occur in the power system over time, the proposed system will try to detect the real-time value of the harmonics distortion.

The purpose of this thesis is to build and test a system that can analyze the harmonics in a single phase electric signal. This system will be based on fast Fourier transform (FFT).

1.4 Organization of this Thesis

This thesis gives a comprehensive description about the developed system, and is organized as follows:

- Chapter 1 begins with an introduction to the research and the idea behind it.
- The second chapter provides insight about related works in the field of Harmonics detection and analysis.
- Chapter 3 gives details about Harmonics detection and analysis.

- Chapter 4 is mostly dedicated to system development, and explains in detail how it operates.
- In the last chapter of this thesis, concluding remarks are stated. Future work, which may follow this study, is also presented.

Chapter 2 - Literature Review

2.1 Background

Power quality can be illustrated as a set of electrical boundaries allowing equipment to operate normally with no serious loss of performance or life expectancy. Numerous methodologies and techniques were intended to increase the power quality. A power system is ideal when a perfect sinusoidal voltage signal is seen at load-ends. Practically, such idealism is very difficult to maintain. Any change from the perfect sinusoidal waveform could cause harmonic distortions. Harmonics are voltages or currents with frequencies which are integer multiples of the fundamental frequency [4].

2.2 Basics and Classification of Harmonics

The voltage and current waveforms differ greatly from a sinusoidal waveform in a real power system. These waveform differences are the Harmonics. For example, if the fundamental frequency of the system is 100 Hz then its 2^{nd} and 3^{rd} harmonic would have frequencies of 200 Hz and 300 Hz respectively [5].

Voltage and current harmonics and harmonics orders are the most used concepts to describe harmonics. Table 1 shows harmonic orders:

Table 1 Harmonic Orders

	Harmonic Orders
Odd	5^{th}, 7^{th}, 11^{th}, 13^{th}, 17^{th}
Even	2^{nd}, 4^{th}, 6^{th}, 8^{th}, 10^{th}, 12^{th}
Triplen	3^{rd}, 9^{th}, 15^{th}, 21^{st}

Generally, even harmonics get cancelled due to their symmetrical nature. However, odd harmonics must be reduced by some filtering techniques [6].

2.3 Past Research

Marvelous work has been done for harmonics, from analyzing them to mitigating them by using different techniques. To get a reliable and efficient functionality of any proposed electrical system, it must be accurately designed. For this purpose, capacitors are utilized as passive filters, which minimize total demand distortion (THD), improve power factor, and eliminate power factor penalties [4].

Lucian Asiminoae, Sergej Kalaschnikow, and Steffan Hansen have explained two harmonic detection methods. The methods are selective harmonic compensation and overall harmonic compensation [7]. A creative method is conferred for measuring the individual harmonics of a time-varying frequency. This suggested method is based on a nonlinear, adaptive mechanism. This technique offers the highest degree of accuracy and frequency-adaptivity [8]. David M. McNamara and Alireza K. Ziarani presented a new method of measurement of harmonics of time-varying frequency. It is based on the

adaptive evaluation of the fundamental frequency and its harmonic components of the power signal [9].

Other researchers have created a system with a combination of the ARM9 chip and virtual instrument technology for a real-time harmonic measurement. This system is conferred in a paper that involves a review of many commonly used methods for power system harmonics measurement [10]. Moreover, these methods are compared according to the aspect of frequency identification [11]. Hsiung Cheng Lin developed a strategy of recursive group-harmonic power minimalization for system harmonic and inter-harmonic evaluation in power systems. The proposed algorithm can measure integer harmonic and the inter-harmonics [12].

Harmonic components and harmonic distortion can be calculated by using a distortion meter. This paper presents the harmonic distortion meter based on microcontroller and its software part carries out calculations using discrete Fourier transform (DFT). DFT is used to calculate the amplitude to measure THD in a power system [13]. In another review, the author has explained and discussed sufficient selective harmonic detection methods in frequency domain as well as in time domain like DFT, fast Fourier transform (FFT), SOGI technique, and CDSP-PLL systems [14].

Estimating the fundamental frequency and measuring both harmonics and inter- harmonics of any unknown frequency is not an easy task. However, by utilizing the adaptive notch filter, this task can be done easily. This methodology measures fundamental frequency and harmonic and inter-harmonic components rapidly [15]. In another paper, a harmonic analyzer is executed using FFT on ARM7 core processor (LPC2138). For matching power rating, the supply voltage is set to 6V using the voltage divider. This

harmonic analyzer can analyze harmonics in single phase supply and provides frequency spectrum of harmonics [16].

It is known that harmonics is a very basic measure of power quality. Thus, measuring and computing harmonics are essential for power quality monitoring. A new device to detect and measure harmonics is presented in other research. This device consists of an analog to digital converter (ADC), FFT unit, liquid-crystal display (LCD) unit, and a network communication unit. This methodology adopts field-programmable gate array (FPGA) and a digital signal processing (DSP) processor. Experimental results illustrate that using this device will increase the accuracy and harmonic power flow, which will also be analyzed [17].

Chapter 3 - Harmonics in Details

3.1 Definition of Harmonics

To get a better understanding of harmonics, the Fourier theorem must be understood. According to The Fourier theorem, all non-sinusoidal periodic functions can be expressed as the sum of following terms (i.e. a series):

- A sinusoidal term which is presented at the fundamental frequency.
- Sinusoidal terms (harmonics) whose frequencies are whole multiples of the fundamental frequency.
- A DC component, if applicable.

The nth order harmonic (commonly referred to as simply the nth harmonic) in a signal is the sinusoidal component with a frequency that is n times the fundamental frequency. The equation for the harmonic expansion of a periodic function is presented below:

$$y(t) = Y_o + \sum_{n=1}^{n=\infty} Y_n \sqrt{2}\ \sin(n\omega t - \varphi_n) \quad \textbf{(3.1)}$$

Where:

Y_o: Value of the DC component of the signal

Y_n: RMS value of each harmonic

ω: Angular frequency of the signal's frequency (fundamental frequency)

φ_n: Displacement of the harmonic component at t = 0.

3.2 Harmonic Generation

Harmonics are unwanted currents and/or voltages. They appear at some multiple of the fundamental frequency. The harmonics can exist in three ways [3]:

i. Through the application of a non-sinusoidal driving voltage to a circuit including non-linear impedance.
ii. Through the application of a sinusoidal driving voltage to a circuit including non-linear impedance.
iii. Through the application of a non-sinusoidal driving voltage to a circuit including linear impedance.

3.3 Sources of Harmonic Distortion

The main sources are the non-linear loads such as: rectifiers, inverters, solid-state-controlled static compensators, solid-state voltage regulators, and cyclo-converters [18]. There are many harmonics sources present, but few sources are listed here which play a role as the major sources of harmonics [6].

- **Static Compensators:** If the power source is varying, passive compensators are used at the ends of transmission lines or near sources of fluctuating power to regulate the voltage. Reactors which are switched by Thyristor will generate near about 1% of the 11th harmonic current [6].
- **Power Converters:** Rectifiers have high inductance on the DC side, thus the DC current is almost constant. The output voltage of a rectifier is a square waveform, and a major source for harmonics.

- **Transformer:** Because of saturation characteristics, a small level of harmonic current will be generated by transformers when they are in the steady state. At the beginning, a high level of harmonics will be produced, which is 60% of the transformer current.
- **Rotating Machines:** In rotating machines, harmonic currents can be produced due to asymmetries in the winding pattern. Harmonics arise due to the resultant magnetomotive force in the machine. Due to the magnetic core saturation, harmonic currents are produced.
- **Switched Mode Power Supplies (SMPS):** The most recent electronic devices contain switched mode power supplies. SMPS manages AC or DC input voltage. The SMPS unit generates current pulses that contain a massive amount of harmonics of third and higher order harmonics.

3.4 Harmonic Indices

There are two frequently used harmonic indices utilized for computing the harmonic content of a waveform [6]:

1.Total Harmonic Distortion (THD)

The THD is a measure of the efficient value of the harmonic components of a distorted waveform. This index can be used for either voltage or current.

$$THD = \frac{\sqrt{\sum_{h>1}^{h\,max} M_h^2}}{M_1} \quad \textbf{(3.2)}$$

Where M_n is the RMS value of harmonic component h of the quantity M. M_1 is the RMS value of the fundamental frequency. The THD is related to the RMS value by the following formula:

$$RMS = \left\{\sum_{h=1}^{hmax} M_h^2\right\} = M_1\sqrt{(1 + THD^2)} \quad \textbf{(3.3)}$$

The total harmonic distortion is very beneficial for many applications. It provides reliable indication for how much extra heat generated when a distorted voltage is applied to a resistive load. Moreover, it gives an implication of losses due to current flowing through conductor. However, THD is not an effective indicator of the voltage stress within a capacitor because it is related to the peak value of voltage waveform. The THD is mostly utilized to describe harmonic voltage distortion. Harmonic voltage is usually referred to as the fundamental component of the waveform at a specific sampling time.

- **Total Harmonic Distortion Current (*THDi*)**

  Generally, THDi is the ratio of the root-sum-square value of the harmonic content of the current to the root-mean-square value of the fundamental current.

$$THDi = \frac{\sqrt{\sum_{h=2}^{hmax} I_h^2}}{I_1} \quad \textbf{(3.4)}$$

  Where I_1 is the fundamental current.

- **Total Harmonic Distortion of Voltage (*THDv*)**

  This gives an indication about the total magnitude of the distortion in voltage. It can be computed by calculating ratio of distorted or harmonic voltage to the fundamental voltage. It can be written as:

$$THDv = \frac{\sqrt{\sum_{h=2}^{hmax} V_h^2}}{V_1} \times 100 \quad \textbf{(3.5)}$$

Where V_h is the voltage amplitude of the hth order harmonic, V_1 is the fundamental voltage amplitude.

For a good power quality, *THDv* should be low.

2. Total Demand Distortion (TDD)

The current distortion can be defined by THD value, but this can often be confusing. A small current may have high THD value, but with no significant impact on the system. This is not a critical matter because magnitude of harmonic current is low, even though current distortion is high.

Some investigators have attempted to prevent this difficulty by referring total harmonic distortion to total demand distortion (that is fundamental of the peak demand load current) and performs as the basis for the guidelines in IEEE standard 519 – 1992 recommended practices and requirements for harmonic control in a power system. TDD is the ratio of harmonic current to the full load fundamental current. The full load current can be defined as the total non-harmonic current absorbed by all loads by the system, when the system is on its peak demand. TDD formula in any power system is:

$$TDD = \frac{\sqrt{\sum_{h=2}^{hmax} I_h^2}}{IL} \quad \textbf{(3.6)}$$

Where I_h is the current amplitude of hth order harmonic, and IL is the peak load current at the fundamental frequency consumed by the system.

3.5 The Impact of harmonics in Power Systems

Harmonics have unfavorable effects in power systems. They show economic impacts such as earlier failure of equipment, losses in distribution systems. The Following is the effect of harmonics on power system and its different components:

- **Power Factor:** Harmonic distortion affects the power factor. Power factor diminish with increasing the amount of harmonic distortion. Generally, non-linear loads result in low power factor.
- **Electric and Electronic Equipment:** Essentially, these devices are deliberated as the source of harmonics. These equipment are sensitive to harmonic distortion. They show effects as increase in supply voltage, zero crossing noise, malfunction of protective devices etc.
- **Conductors:** Usually, heat will be produced in the current carrying conductors due to I2R losses (Copper losses). Moreover, heating of conductors may arise because of the magnetic field of harmonic currents in the adjacent conductors.
- **Transformers:** Frequency causes Eddy current losses. Eddy currents produce resistive losses that convert some forms of energy, such as kinetic energy, into heat. Thus, as the harmonic order increases, eddy current losses for transformers also increase. Moreover, eddy current losses in transformer will fallout in overheating and the transformer would be defective.

- **Capacitance:** The Capacitors enhance the power factor. They have an important influence on harmonic levels. As the frequency of harmonics increases, the capacitive reactance decreases.
- **Circuit Breakers and Fuses:** Low level faults in circuit breakers occur due to the high degree of harmonic load current. High $\frac{di}{dt}$ ratings at zero crossings for sinusoidal waveform make the disruption complex, for load distortion. So, harmonic load currents result in circuit collapse.
- **Telephone Interferences:** Fundamental frequency doesn't cause any major problems. However, power system harmonics can cause serious problems because human audible sensitivity and telephone response peak have near 1 KHz. Inductive, capacitive and conductive interferences can take a place between telephone line and a power line.

3.6 Harmonic Power

Harmonic powers (including the fundamental) add and subtract independently to generate total average power. Average power is defined as [19]:

$$P_{avg} = \frac{1}{T}\int_{t}^{t+T} v(t)i(t)dt \quad \textbf{(3.7)}$$

By substituting the Fourier series for the voltage and current in (3.7), the average value of all the sinusoidal terms becomes zero, leaving only the time invariant terms in the summation, or

$$P_{avg} = V_{dc}I_{dc} + \sum_{k=1}^{k\ max} V_{k,rms} \cdot I_{k,rms} \cdot dpPf_k = P_{dc} + P_{1,avg} + P_{2,avg}, \dots, P_{k,avg} \quad \textbf{(3.8)}$$

Where $dpPf_k$ is the displacement power factor for harmonic k.

The harmonic power terms are mostly losses and are generally small according to the total power. However, harmonic losses may sometimes be a significant part of total losses. According to (3.8), if there is no harmonic voltage at the terminals of a generator, then the generator produces no harmonic power. However, because of the non-linear loads, harmonic power does occur in power systems and produces additional losses.

3.7 True Harmonic Factor

Voltage and current harmonics that are generated by non-linear loads, increase power losses and have a negative impact on electric utility distribution systems and components. While the specific relationship between harmonics and losses is not simple and hard to generalize, the absolute concept of power factor does provide some measure of the relationship, and it is beneficial when comparing the relative effects of non-linear loads, providing that harmonics are integrated into the power factor definition. True power factor is defined as [20], [21];

$$pf_{true} = \frac{P_{avg}}{V_{rms}\ I_{rms}} \tag{3.9}$$

When the voltage and current waveforms are both sinusoidal, (3.9) reduces to the familiar displacement power factor,

$$dpPf_1 = \cos(\theta) \tag{3.10}$$

Where θ is the angle between the fundamental voltage and current.

When harmonics are present, (3.10) can be expanded as;

$$pf_{true} = \frac{P_{1,avg} + P_{2,avg} + P_{3,avg} \ldots\ldots}{\left(V_{1,rms} \sqrt{1+THD_v^2}\right) \cdot \left(I_{1,rms} \sqrt{1+THD_I^2}\right)} \quad \textbf{(3.11)}$$

A beneficial simplification to (3.11) is achieved by making two assumptions:

1. In most cases, the contributions of harmonics above the fundamental to the average power may not be that important. Hence, $P_{avg} \approx P_{1,avg}$.

2. Since THD_v is normally less than 10%, $V_{rms} \approx V_{1,rms}$

Combining these two assumptions into (3.11) yields the following approximate form for true power factor:

$$pf_{true} = \frac{P_{avg}}{\left(V_{1,rms} \; I_{1,rms} \; \sqrt{1+THD_I^2}\right)} = dpf_1 * \; pf_{dist} \quad \textbf{(3.12)}$$

It is clear in (3.12) that the true power factor of a nonlinear load is limited by its THD_I. Single-phase power electronic loads tend to have high current distortions. Thus, their true power factors are lower than unity (i.e. 1), even though their displacement power factors are near unity.

Chapter 4 - Harmonics Detections System Modeling and Simulations

4.1 Data Collection

The following signals are used in the analysis:

1. **Signal A**: An Ideal artificial 60Hz signal with no electrical noise (Harmonics). This signal was generated using MATLAB. The signal has 2048 data points. Each point has a value of time and a value for magnitude of voltage at that time.
2. **Signal B**: A 60Hz artificial signal with electrical noise (Harmonics). This signal was also generated using a MATLAB code. This signal has 2048 data points. Each point has a value of time and a value for magnitude of voltage at that time.
3. **Signal C**: A 60Hz signal with low noise (Harmonics) from a house receptacle, taken using an oscilloscope. This oscilloscope recorded 2000 points. Each point has a value of time and a value for magnitude of voltage at that time.

4.2 Software

Three Main software programs are used in the development of the proposed system:

- MATLAB R2017a (**mat**rix **lab**oratory) is utilized in writing the codes of the system. MATLAB is a very high- performance language for technical computing.

It is a fourth-generation programming language generated by MathWorks. MATLAB allows matrix manipulations, plotting of functions and information, use of algorithms, development of user interfaces, and dealing with programs and scripts written in other languages including C, C++, Java, VHDL, and Python [23]. It merges computation, visualization, and programming in an easy-to-use environment where issues and their solutions are expressed in known mathematical notation.

- Altera Quartus II 15.0 is a programmable logic device design software developed and designed by Altera®. Quartus II software has many features, including SOPC Builder, SoCEDS, external memory interface toolkit, and Qsys. Qsys is a system integration tool that is the next generation of the SOPC Builder. It uses an FPGA-optimized network-on-chip-architecture. In this thesis, Qsys is used to generate Altera® Fast Fourier Transform II (FFT MegaCore) that includes Bit-accurate MATLAB models. It supports analysis and synthesis of HDL design, which allows engineers and developers to compile and run their designs and execute timing analysis. Quartus includes an implementation of VHDL or Verilog for hardware description, visual editing of logic circuits, and simulation of vector waves compilation.
- The FFT MegaCore function is a high performance, highly-parameterizable Fast Fourier Transform processor. This function was used heavily during the development of this thesis. More details about this functionality will be presented and explained in this chapter. MATLAB is capable of converting its codes into VHDL codes using the HDL coder toolbox. HDL coder generates portable,

synthesizable VHDL code from MATLAB functions. This code can be used for the FPGA programming. HDL coder provides a workflow advisor that automates the programming of Altera® FPGA. HDL architectures and implementation can be modified, highlight critical paths, and generate hardware resource utilization estimates. HDL Coder offers traceability between your Simulink model and the generated VHDL code, enabling code verification for high-integrity applications.

4.3 System Datasets and Parameters

In this thesis, two signals were generated using MATLAB and one signal was recorded using an oscilloscope. The two generated signals consist of 2048 data-points, and the recorded signal consists of 2000 data-points. Each point has 2 values: the time and the magnitude of voltage at that time. The system is implemented and tested using MATLAB R2017a, and an Altera® FFT MegaCore function powered by Qsys. The laptop used in the system processing and computation of the signals is a HP Zbook laptop with an Intel® Core™ i7-4810MQ CPU 2.80GHz, 16.0 GB RAM, 64-bit operating system, and Windows 8.1. In this thesis, 6096 samples were used: 2 artificial signals of 2048 data-points each, plus one signal of 2000 data-points ((2 x 2048) + (1 x 2000)).

4.4 System Block Diagram

The Harmonics detection process in the proposed system consists of multiple steps. Figure 1 shows the diagram that summarizes these steps.

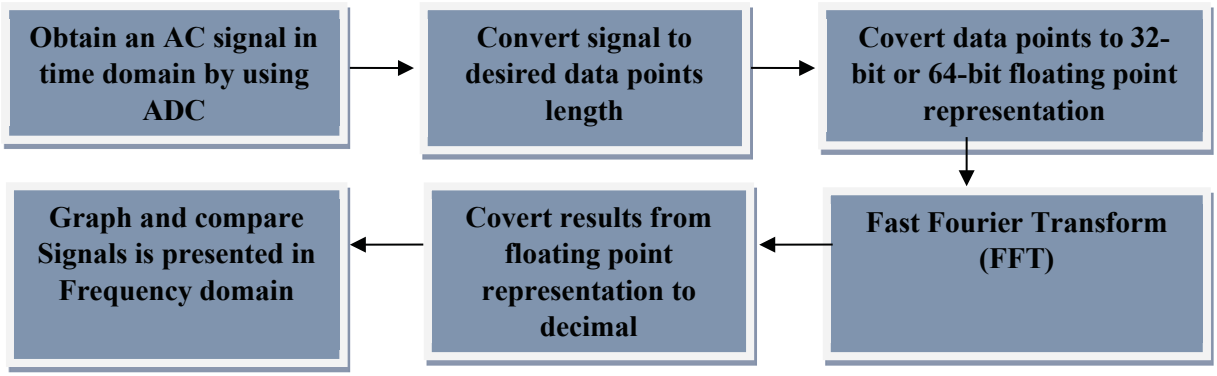

Figure 1 Harmonics Detection Process

In the first stage of the process, an AC signal is obtained by using an ADC (Analog-to-Digital Converter). Another way of obtaining signals is to artificially generate them, using software such as MATLAB. This technique allows engineers to simulate and test desired input signals. This method is convenient because it generates the signal to exact desired data points.

When the signal is recorded, the next step is to make the data compatible with the proposed system's parameters. The proposed system is capable of testing 2048 data-points, which might not be the number of points for the recorded data. In that case, two actions should be taken:

i. If the number of data-points is more than the system's size (2048 data-points), the signal is shortened by taking a 2048 points segment of the signal, or by taking larger sampling intervals.

ii. If the number of data-points is less than the system's size (2048 data-points), zero padding is performed to adjust the signal's size to the 2048 points. Zero Padding indicates adding zeros to the end of a time-domain signal to enlarge its length.

In the data converting stage, numbers are converted to single precision floating-point (32-bit) since that is the representation format that is compatible with FPGA.

IEEE Standard 754 floating point is a common representation of numbers for processors and computers, floating point representation uses scientific notation to encode numbers [24]. Floating point representation solves various numbers of problems that would face developers and engineers using other types of representations such as fixed-point representation. Fixed-point representation has a fixed frame of representation which limits it from being accurate when representing very small or very large numbers. In addition, fixed-point representation tends to lose accuracy and precision when two large numbers are divided. On the other hand, floating-point applies a "sliding frame" of precision, which allows a representation of very large and very small numbers with maximum precisions. There are two types of floating-point representations, single precision (32-bit) and double precision (64-bit) [24].

In the FFT stage, fast Fourier analysis is performed on the time-domain signal to convert it to frequency-domain. The frequency-domain representation of a signal includes information about the input signal's magnitude and phase at each frequency. This is why the FFT output computation is complex. FFT will be further explained in section 4.4.1

After performing the FFT on the input data, the output is in floating-point representation. Therefore, the next step is to convert the output back to decimal representations to be able to graph the data using graphing tools. The graphing tool used and implemented in this project is MATLAB.

4.4.1 Fast Fourier Transform (FFT)

The FFT is an efficient way of calculating the Discrete Fourier Transform (DFT). DFT is identical to Fourier transformation in continuous signals. It is, however, used to transform a discrete signal to discrete frequency spectrum [25]. Based on Nyquist sampling theorem, the maximum frequency that can be noticed in frequency domain is one half the sampling frequency. In this thesis, three signals were implemented. Two signals are sampled at 40960 HZ sampling rate, and one is sampled with 40000 Hz. After performing the FFT, the maximum expected frequency in the spectrum will be 20480 Hz, and 20000 Hz respectively.

The Fourier Transform has endless applications ranging from speech recognition, to astronomy, to Radar, and to mobile phones. Thus, it is one of the most useful mathematical techniques ever created. For transforming the discrete-time signal from time-domain into its frequency-domain, the FFT is nothing but the DFT. The difference is that the FFT is faster, more effective, and more accurate on calculations. Hence, it is appropriate to consider FFT by firstly considering the N-point DFT equation which is given by:

$$X(k) = \sum_{n=0}^{N-1} x(n)\, e^{jw_k n} \qquad \textbf{(4.1)}$$

Where *x(n)* is the input, $e^{jw_k n}$ is the phase factor, and *n* and *k* are integers from *0 to N-1*. Initially, separate *x(n)* into two portions*: x(odd)=x(2m+1)* and *x(even)=x(2m),* where m=0,1,2,…,N/2-1. Then the N-point DFT equation also becomes two parts, and ends up with the following equation:

$$X(k) = \sum_{m=0}^{\left(\frac{N}{2}\right)-1} x_1(m)\, \boldsymbol{W}_{N/2}^{mk} + \boldsymbol{W}_N^{mk} \sum_{m=0}^{\left(\frac{N}{2}\right)-1} x_2(m)\, \boldsymbol{W}_{N/2}^{mk}$$

$$= X_1(k) + \boldsymbol{W}_N^k X_2(k) \quad , \boldsymbol{k=0, 1, \ldots N/2} \tag{4.2}$$

$$X\left(k+\frac{N}{2}\right) = X_1(k) - \boldsymbol{W}_N^k X_2(k) \, , \boldsymbol{k=0, 1, \ldots N/2}$$

Where $e^{jw_k n} = \boldsymbol{W}_N^{kn}$. Here the N-point DFT is separated into two N/2-point DFT. For original N-point DFT Eq. (4.1), it has (N^2) complex multiplications and N/2-point DFT Eq. (4.2) has $(N^2/2) + (N/2)$multiplications. This is the operation for minimizing the calculations from N points to N/2 points. This signal for N point DFT is continuously subdivided until the final signal sequence is reduced to the one-point sequence. So, the total number of complex multiplications will be approximately reduced to (N/2) log_2(N) [26].

The FFT returns a set of complex numbers (amplitude and phase), with exception of the spectral components at *f=0 and f=fs/2 (Nyquist Rate)*. DFT has linearly spaced frequency bands, as its bins are spaced at intervals of (Fs/N), where N is the length of the DFT vector (number of points), and fs is the sampling rate. The MATLAB command that was used to acquire the FFT is fft(x). This command calculates the DFT of x using a fast Fourier Transform algorithm. To determine the magnitude values of the FFT output, abs (fft(x)) will return the magnitude only and we need to start analyzing signals. It was performed at 2048-point DFT on the time-domain samples using MATLAB and Altera® Quartus II (FFT MegaCore function).

The FFT MegaCore function implements a complex FFT or inverse FFT (IFFT) for high-performance applications. The FFT MegaCore function implements the following architectures:

- Fixed transform size architecture.
- Variable streaming architecture.

The FFT MegaCore function is included in Altera® Quartus II libraries under DSP library. The proposed system specifications are showed in the table below:

Table 2 FFT MegaCore function Parameters

Function Parameters	Values
Transform Length	2048 points
Transform Direction	Forward
I/O Data Flow	Variable Streaming
Input Order	Natural
Output Order	Natural
Data and Twiddle Representation	Single Floating Point
Calculation Latency	2048 cycles
Throughput Latency	4096 cycles

The basic step, while configuring FFT MegaCore function parameters, is to determine the transform length. Transform length shows the maximum transform length that can be performed. 2048 points were chosen as transform length. Transform direction is specifiable on a per-block basis through an input port and in this thesis, it was specified in the forward direction.

The streaming I/O data flow FFT architecture allows continuous processing of input data, and outputs a continuous complex data stream without the requirement to cutoff the data flow in or out of the FFT function.

The variable streaming architecture FFT implements a radix-2^2 single delay feedback architecture, which a developer can configure during runtime to perform the FFT algorithm for transform lengths of 2^m, where $4 \leq m \leq 18$. This architecture implements either a fixed-point representation or a single precision floating-point representation. In this research, the architecture used a single precision floating point that allows a large dynamic range of values to be represented while controlling a high Signal to Noise Ratio (SNR) at the output. Radix-2^2 single delay feedback architecture is a fully pipelined architecture for computing the FFT of incoming data. It is like radix-2 single delay feedback architectures. There are $log_2(N)$ stages, with each stage containing a single butterfly unit and a feedback delay unit that delays the incoming data by a specified number of cycles, halved at every stage where N is the transform length [26].

4.5 **The Proposed System (FFT IP Core System)**

This system was constructed to process the signals and perform Fast Fourier Transform on them using VHDL. VHDL is a shortcut for VHSIC Hardware Description Language, which is a hardware-description language capable of re-using components to make complex designs highly repeatable with quick design times. VHDL designs and codes can be implemented on Field-Programmable Gate Array (FPGA), which allows engineers to emulate their designs. Altera is a manufacturer of Programmable logic devices (PLDs) and it is one of the biggest FPGA's Companies. Altera also have a PLD design software called Quartus II and a simulation software called Modelism. Both software are used heavily in the proposed system.

Altera offers an array of Intellectual Property (IP) cores that work as building blocks for developers and engineers, where they can use these IP Cores in their systems to perform special functions. IP cores save engineers a lot of time and prevent them from having to create the same design block for every project from scratch. There are many IP cores that Altera provides for various functions such as finite impulse response (FIR) II for filtering applications, numerically controlled oscillator (NCO) for signal generations applications, and FFT for transforms applications. Even though Altera provides the IP core, the significant part of the design is to put the IP core in a system to be able to make it function correctly.

In the proposed system, an Altera FFT IP core was used to perform fast Fourier transform on the signals. FFT IP function can be parametrized to use either quad-output or single-output engines. Quad-output refers to processing ability of the internal FFT butterfly processor, quad-output FFT engines minimize transform time by computing four radix-4 butterfly complex outputs in every clock cycle. Single-output FFT engine also refers to the proceeding ability of the internal FFT butterfly processor, which is a single butterfly output per clock cycle, requiring one complex multiplier. In the proposed system, a quad-output FFT engine is used to keep the process time as short as possible. A single-output engine can be used in the proposed system; however, it would increase the process time to four times the current process time. A single-output engine will require only one complex multiplier which means the system will use less random-access memory (RAM) and will require a lower performance FPGA.

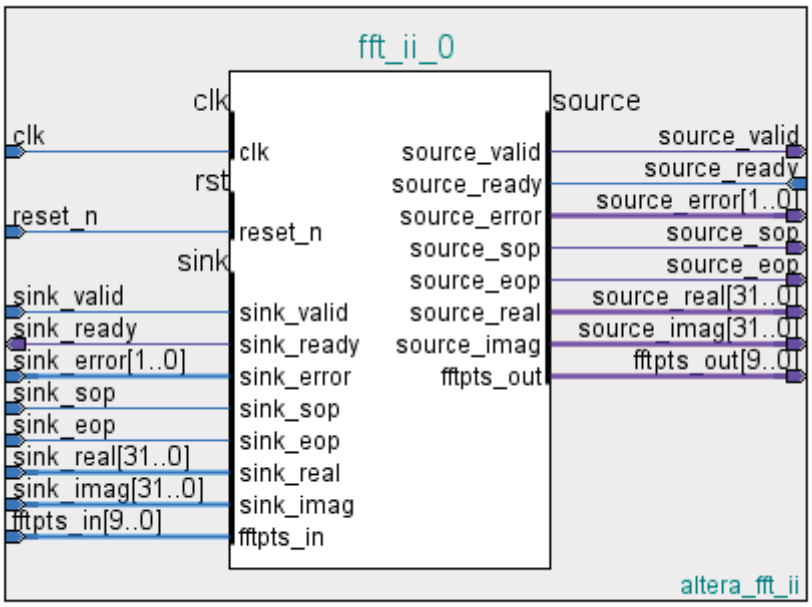

Figure 2 FFT IP Core Block Symbol

Figure 2 shows the block symbol for FFT IP core with the input and output signals.

On the input side:

- Clk: clock signal that clocks all the engine components.
- Reset_in: an active low asynchronous reset signal.
- Sink_eop: this signal announces the end of the incoming FFT frame.
- Sink_error: announces when an error exists in the upstream module.
- Sink_imag: imaginary data input.
- Sink_real: real data input.
- Sink_valid: indicates when the incoming data bus is valid.
- Sink_data: a variable signal includes the inputs data signals from most significant bits (MSB) to least significant bits (LSB) for Sink_real, sink_imag, and fftpts_in.

- Source_ready: affirms when the module can accept data again confirmed by the downstream.

On the output side:

- Sink_ready: indicates when FFT engine can accept data.
- Source_eop: spots the end of the outgoing FFT frame.
- Source_error: indicates when there is an error in the upstream module or in the FFT module.
- Source_exp: accounts for scaling the internal signal values during the FFT Process.
- Source_imag: imaginary data outputs.
- Source_real: real data outputs.
- Source_sop: spots the start of the outgoing FFT frame.
- Source_valid: indicates when there is valid data to output.
- Source_data: a variable signal includes the output data signals from most significant bits (MSB) to least significant bits (LSB) for source_real, source_imag, and fftpts_out.

FFT IP core only takes values in floating-point representation, which also sends outputs in the same representation format. Therefore, a significant part of design was to enable the system to convert the inputs from real values representation to floating-point representation. Also, converting the outputs form floating-point representation back to real value representation. For this purpose, a VHDL code was written to be a part of the system and to perform these two main tasks. Another significant part of the design was to correctly

time the inputs and the outputs with the IP Core clock: one input and one output every clock cycle. For that purpose, a tool command language (TCL) script was written to time inputs and outputs and make the simulation using ModelSim Possible. Figure 3 shows a simplified diagram of the proposed system. The diagram shows how inputs are first converted to floating-point representation, processed through the FFT IP core, and then converted back to decimal representation. After the data is converted back to decimal representation, the data is then graphed and simulated to compare to the actual results which we get from MATLAB.

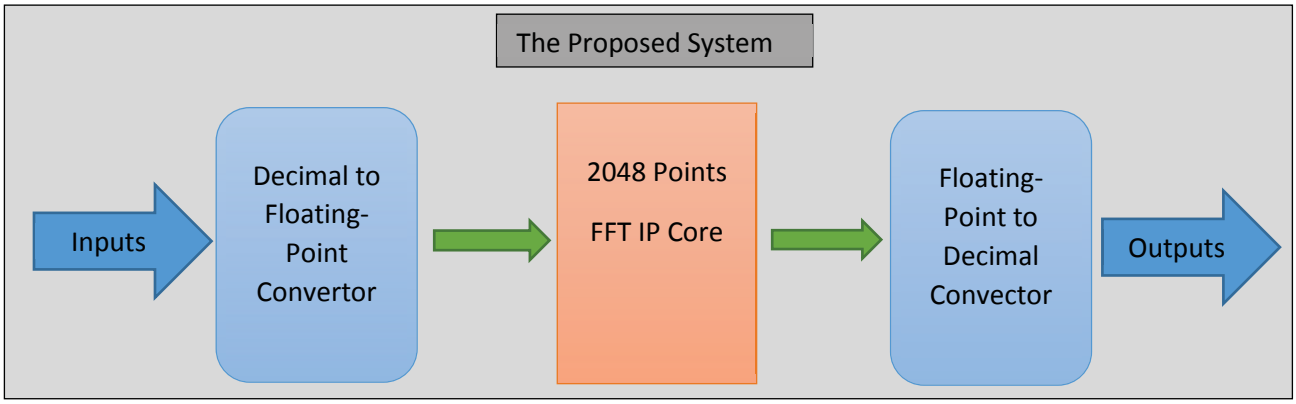

Figure 3 Simplified Diagram of the Proposed System

4.6 Signal Analysis

In this section, the three signals (A, B and C) are simulated and analyzed to understand their characteristics and to compare between the theoretical results (MATLAB) and the actual results (FPGA) for each of the three signals.

4.6.1 Signal A

As previously mentioned in this chapter, signal A is an ideal artificial 60Hz signal with no electrical noise. Signal A is constructed using MATLAB and it consists of 2048 points. The following table demonstrates the characteristics of signal A. This signal was

sampled with 40960Hz sampling frequency, the number of wave cycles are 3, and the number of data points are 2048. The amplitude was recorded to be 170 volts.

Table 3 Characteristics of Signal A

Signal Characteristic	Value
Frequency of main wave	60Hz
Number of Periods/Cycles	3
Number of data points	2048
Amplitude of wave	170
Sampling rate	40960

Figure 4 shows signal A in time domain. Time domain refers to the variation of voltage amplitude of the signal with time. It can be noticed from the figure that the signal is smooth and not distrusted by harmonics. FFT was performed for signal A using both FPGA and MATLAB. The signal was first processed and simulated on the FPGA using ModelSim. Each value of the 2048 Values was processed and the output was 2048 values as well. The output was constructed of 2048 real values and 2048 imaginary values. Figure 5 and figure 6 show how the inputs were processed and the how the output values were demonstrated. In figure 5, it is noticed how signal sink_valid changed from high to low, indicating that the incoming data is valid and can be processed. Another change can be noticed in the sink_eop signal, as the signal changes to high then back to low again, announcing the end of the incoming FFT frame.

In figure 6, the change in signal Source_valid can be seen, this change indicates that there is valid data to output. Another change can be noticed in signals Source_sop and Source_eop. These two signals spot the start and the end of the outgoing FFT frame.

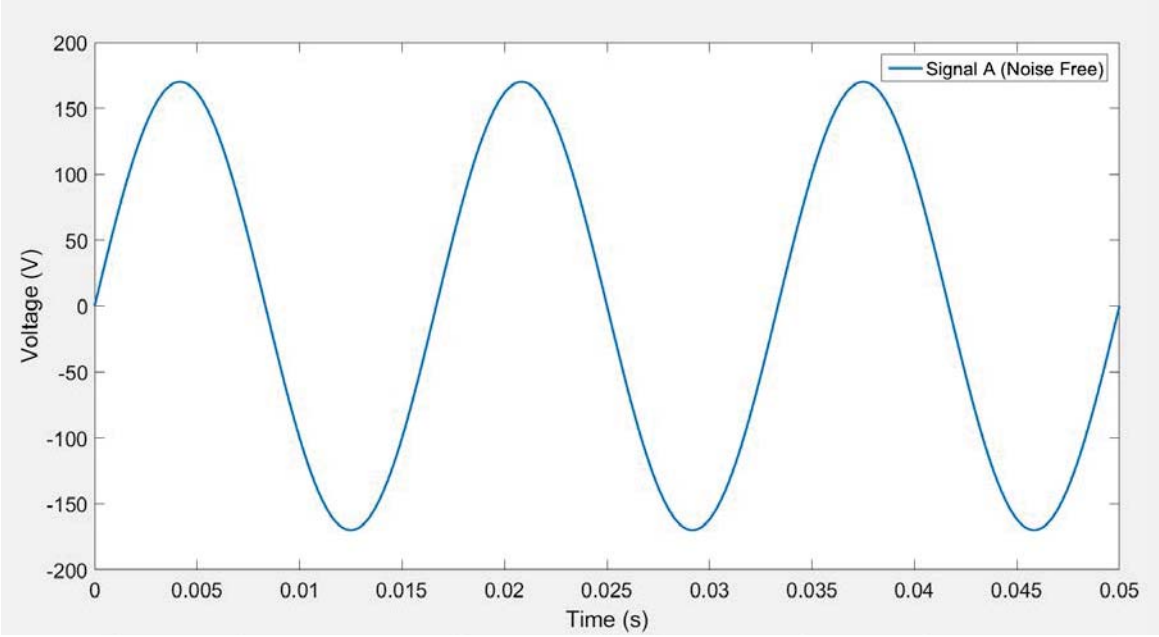

Figure 4 Signal A in Time Domain

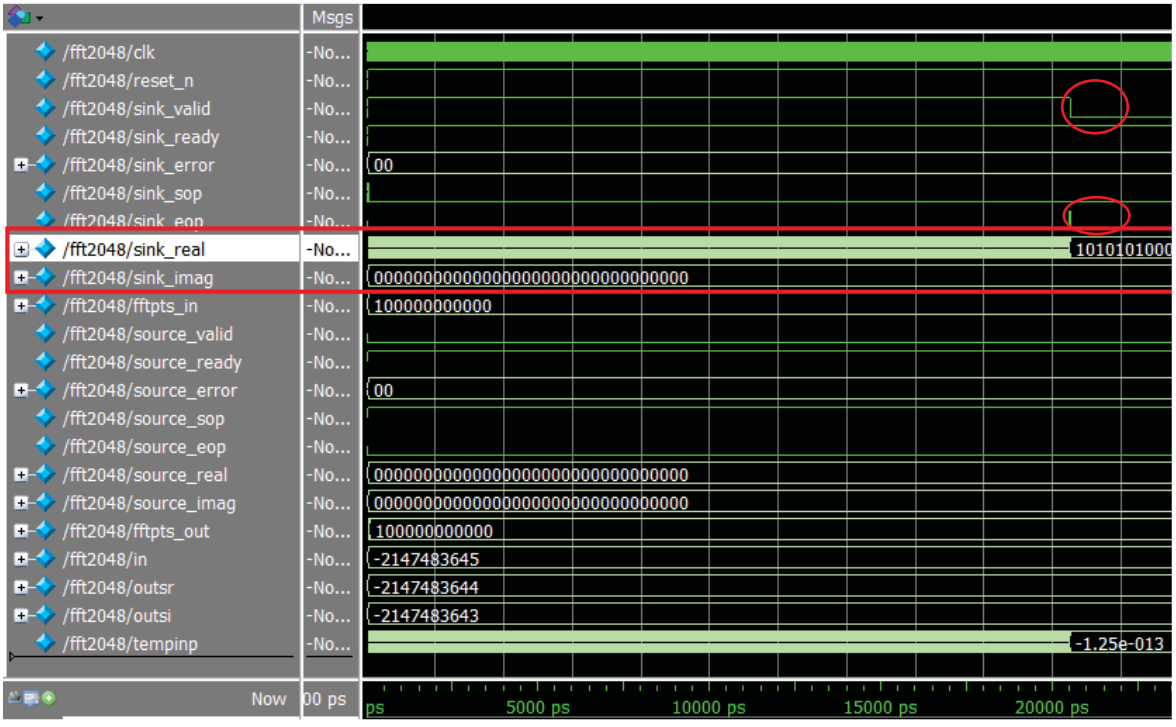

Figure 5 Signal A Inputs Being Processed in Modelsim

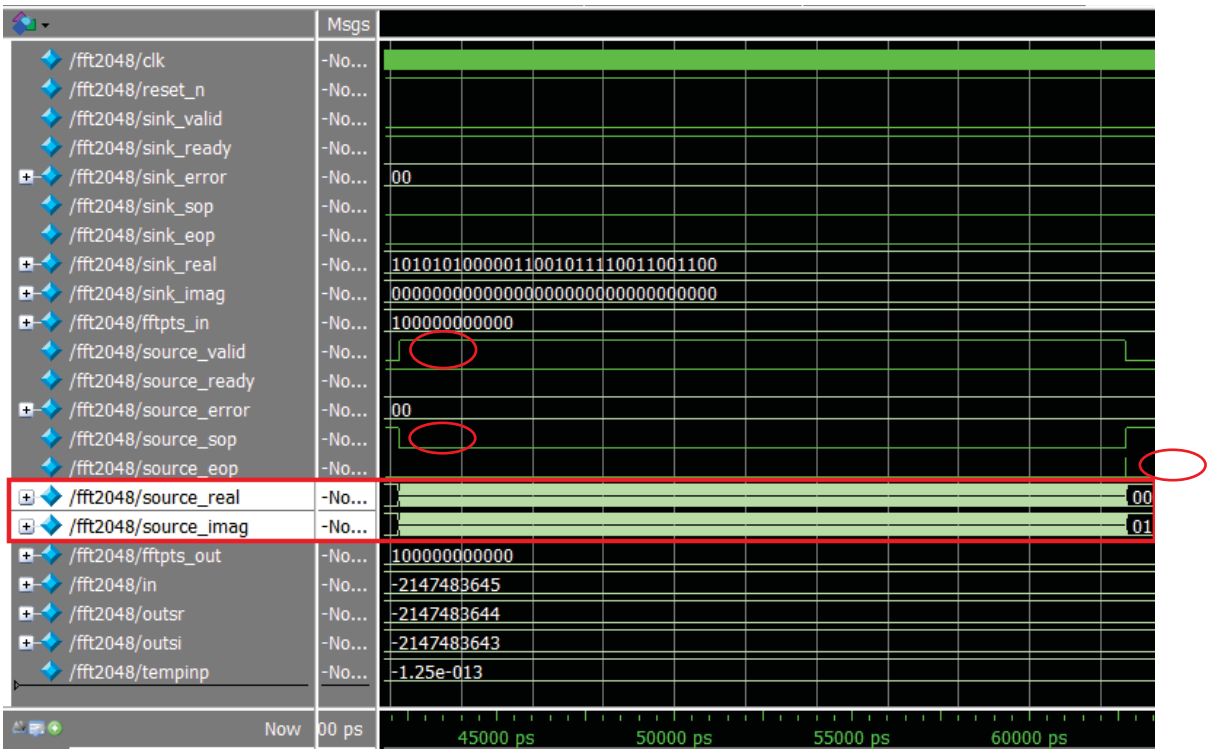

Figure 6 Signal A Outputs from Modelsim Simulation

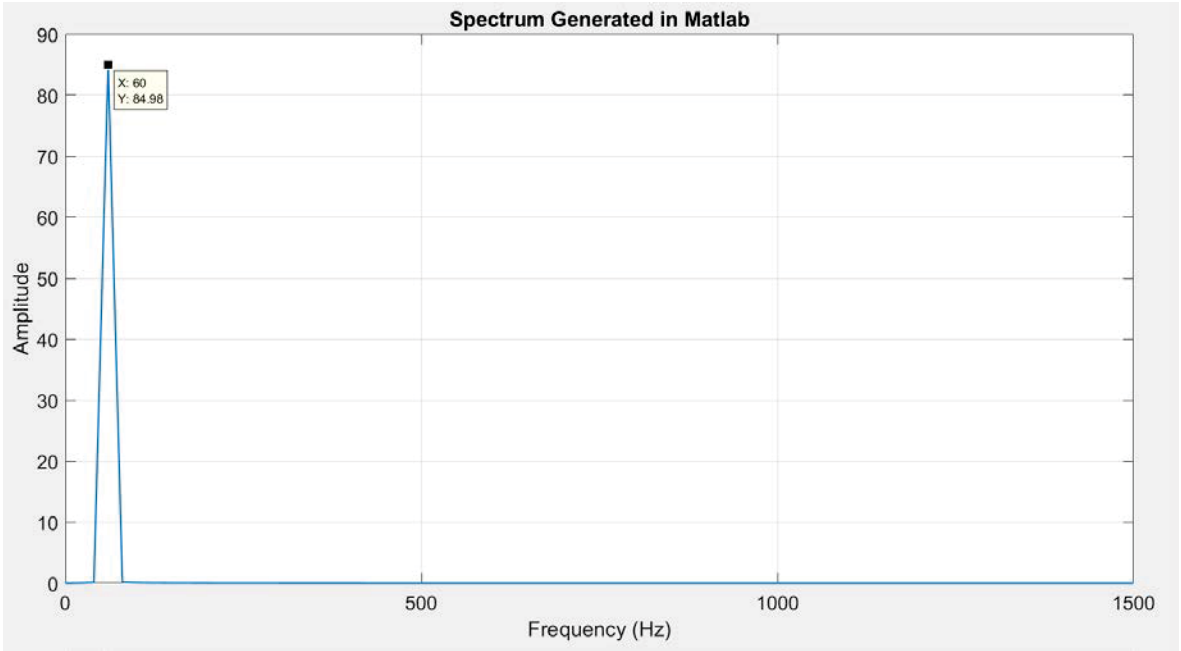

Figure 7 FFT Spectrum for Signal A Generated in MATLAB

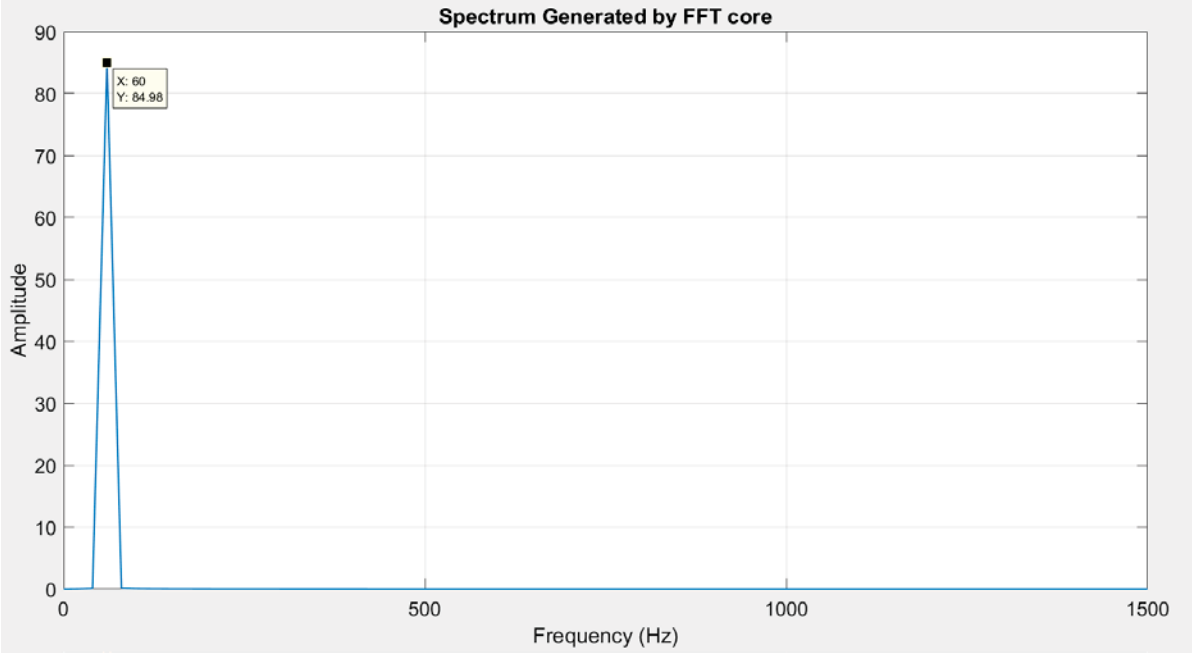

Figure 8 FFT Spectrum for Signal A Generated by FFT IP Core

After processing the signal's values through the proposed system, the two output files (real & imaginary) were graphed using MATLAB to get the signal in the frequency domain. As mentioned, fast Fourier transform was performed on the signal separately using MATLAB to get the Theoretical values. The two graphs were then compared to see if the theoretical value matches the actual value.

As shown in figure 7 and figure 8, the first fundamental frequency is at 60Hz exactly and the amplitude of the fundamental frequency equals 84.98 in both graphs. Therefore, MATLAB results match the FFT Core (FPGA) results, which means that the proposed system is functioning ultimately as it's supposed to in computer simulation.

4.6.2 Signal B

Signal B is also a 60Hz artificial signal. However, unlike Signal A, signal B has electrical noise (Harmonics). White Gaussian Noise was also added to the signal to make the noisy signal as close as possible to a realistic situation. The signal was constructed using MATLAB and it consists of 2048 points. The following table demonstrates the characteristics of signal B. Signal to Noise Ratio (SNR) is the ratio of a signal's power versus a level of noise power and usually expressed as a measurement of decibels (dB). Decay Rate refers to how fast the harmonics decay. If the decay rate is 0, all the harmonics would have the same amplitude.

Table 4 Characteristics of Signal B

Signal Characteristic	Value
Frequency of main wave	60Hz
Number of Periods/Cycles	3
Number of data points	2048
Amplitude of wave	170
Sampling rate	40960
Signal to Noise Ratio (SNR)	3.5
Number of Harmonics	9
Decay Rate	1
Power of white Gaussian noise	1 dBW , 1 W

Figure 9 shows signal B compared to signal A in time-domain. It can be noticed in the figure how the sinusoidal wave in signal B is not smooth and consistent due to the existence of harmonic distortion. On the other hand, signal A is stable and consistent since there are no harmonics disturbing the signal.

Figure 10 shows a zoomed section of signal A and B in Time-Domain showing how White Gaussian Noise is affecting signal B. It can be noticed in the figure that signal B is not perfectly sinusoidal, and it's also not smooth. White noise is the noise produced

by combining all the different frequencies of sound at once, which explains the non-uniformity seen in signal B.

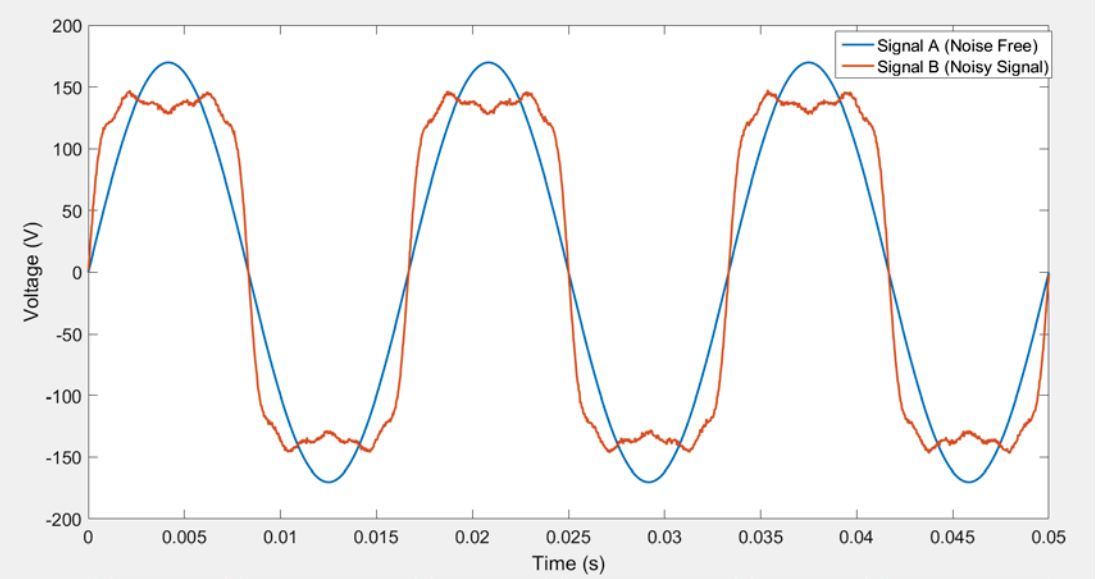

Figure 9 Signal B Compared to Signal A in Time-Domain

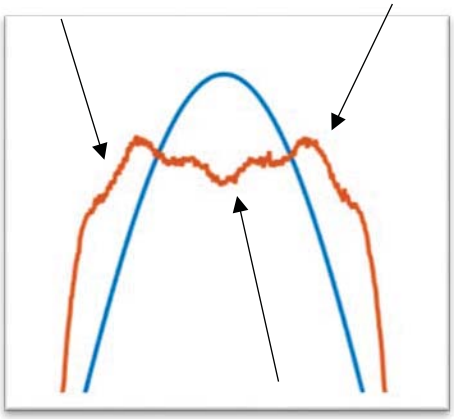

Figure 10 zoomed section of signal A and B in Time-Domain showing White Gaussian Noise

After constructing signal B in MATLAB, the same steps in the previous chapter were taken. First, fast Fortier transform was performed on the signal using FPGA (the proposed system). Results were then graphed and presented. Then fast Fourier transform was performed again using MATLAB and the results were also graphed. Lastly, both graphs were compared to check whether the theoretical results (MATLAB) and the actual

results (FPGA) are equal. Figure 11 shows how inputs were processed using ModelSim and figure 12 shows how the outputs were delivered.

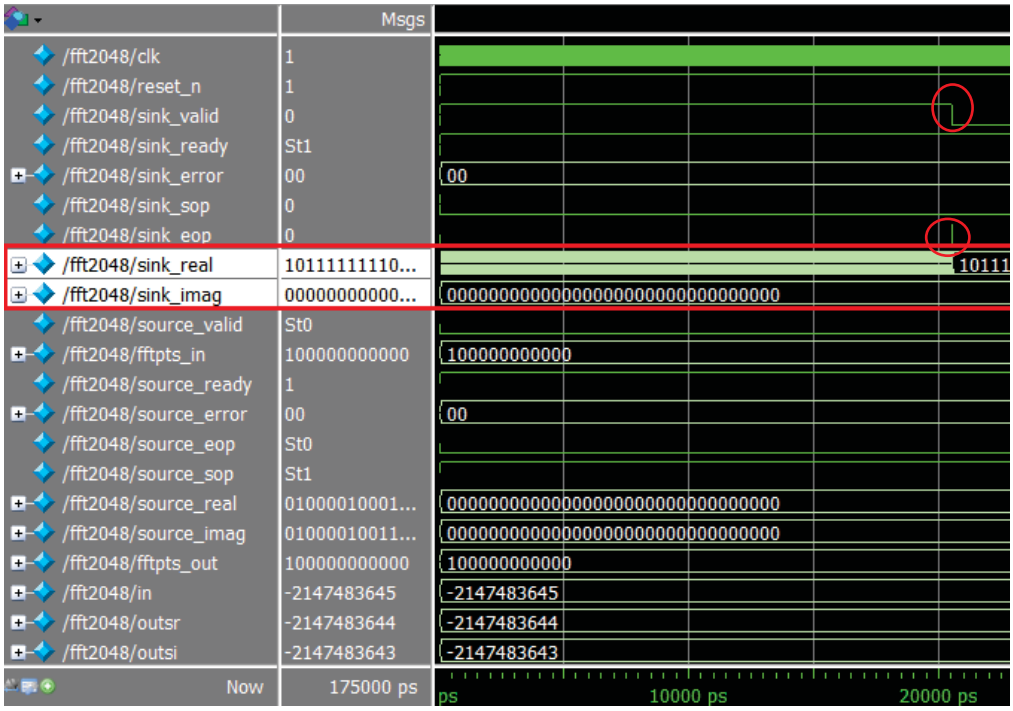

Figure 11 Signal B Inputs Being Processed

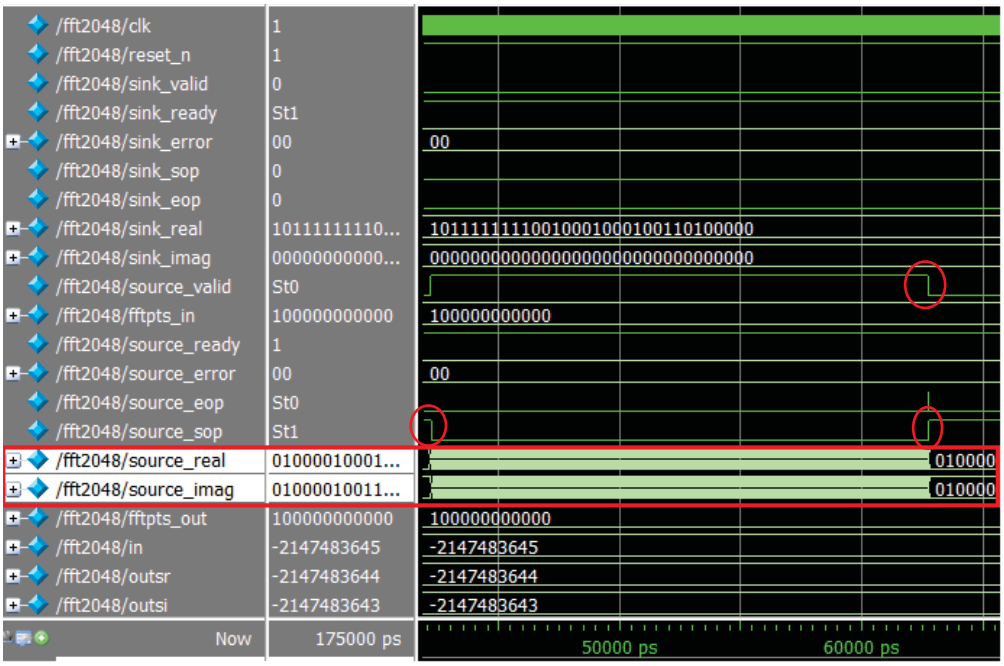

Figure 12 Signal B Outputs

Processing signal B inputs takes around 20505 pico-seconds (ps), and delivering the outputs takes around 42200 ps. Therefore, the whole process timing is about 62715 ps. Results are graphed and compared to the MATLAB results.

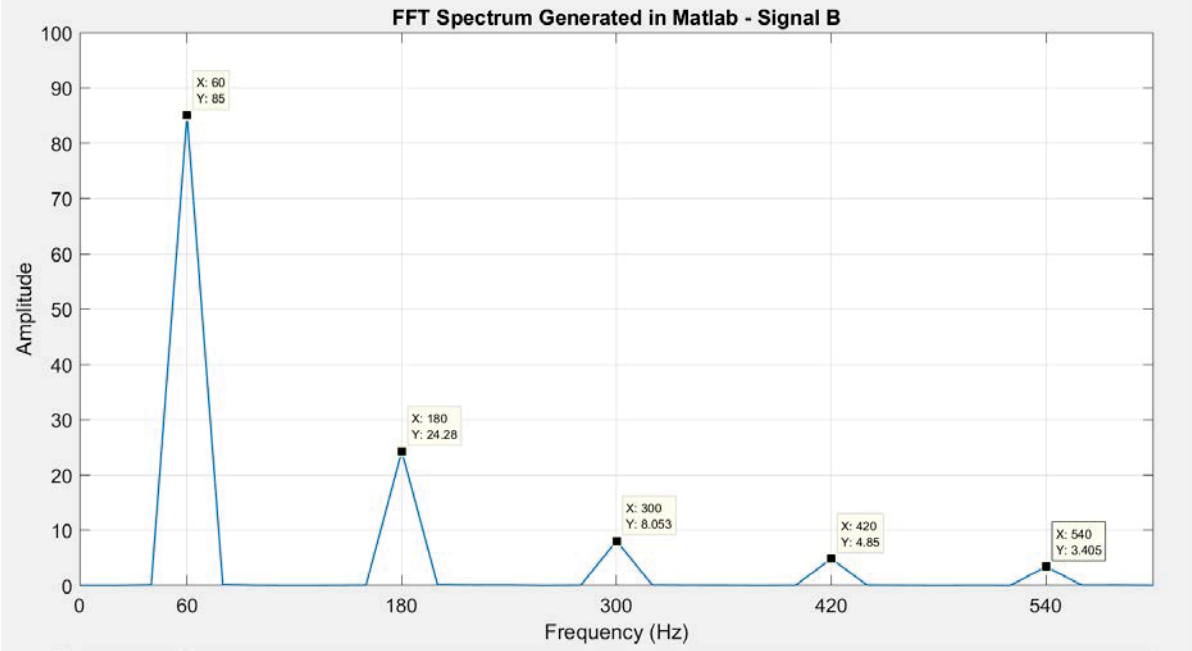

Figure 13 FFT Spectrum for Signal B Generated in MATLAB

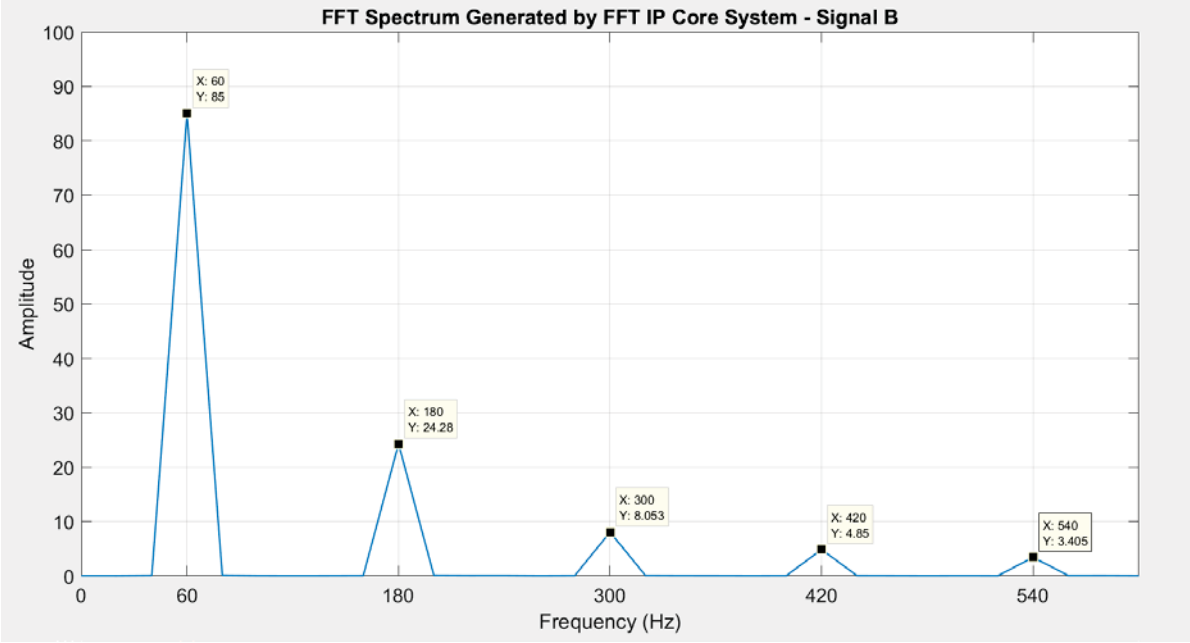

Figure 14 FFT Spectrum for Signal B Generated by FFT IP Core System

Comparing the two graphs in Figure 13 and Figure 14, it is observed that the values for all five harmonics are exactly the same in both graphs. Therefore, the theoretical results equal the actual results, which means that the experiment was successful. The next table lists the frequency and the amplitude for the five harmonics.

Table 5 Amplitudes for Harmonics in signal B

Harmonic	1st	3rd	5th	7th	9th
Frequency	60	180	300	420	540
Amplitude	85	24.28	8.053	4.85	3.405

4.6.2 Signal C

Unlike the signals A and B, signal C is a real 60Hz signal that was recorded from a house receptacle using an oscilloscope, while the other two signals were artificially constructed using MATLAB. Signal C only has 2000 data points and the FFT IP core system requires 2048 points. However, FFT IP core automatically performs zero padding on the signal to get it to the proper size. For signal C, three FFT Spectrum graphs will be presented. The first one for signal C is with 2000 data points without zero padding using MATLAB, and the other two FFT spectrum graphs are for the signal with zero padding using MATLAB and the FFT IP Core system respectfully. Figure 15 shows signal C in time domain, and Figure 16 shows signal C in frequency domain after performing FFT on it without zero padding using MATLAB.

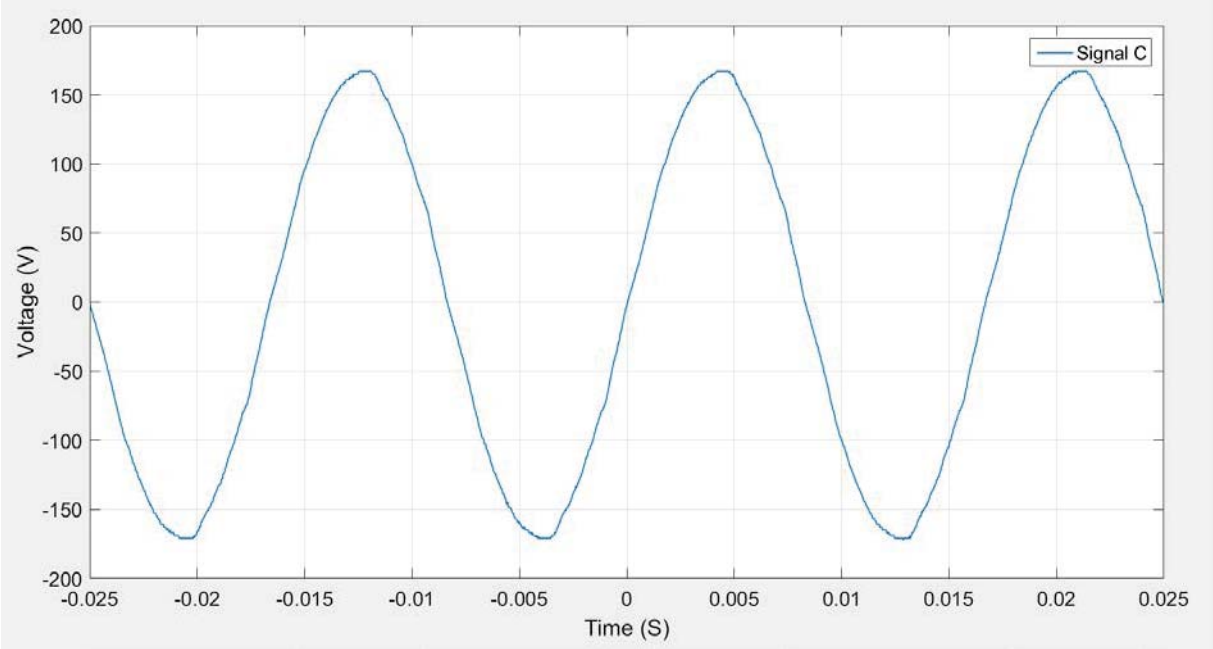

Figure 15 Signal C in Time Domain

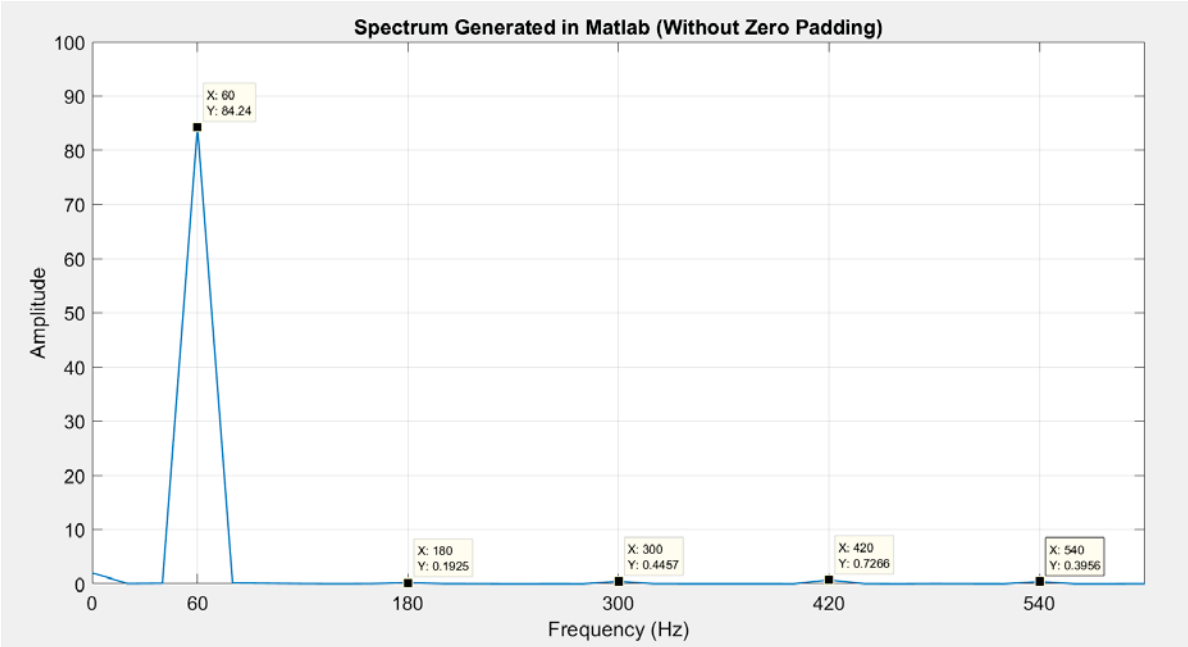

Figure 16 FFT Spectrum for signal C Generated in MATLAB without Zero Padding

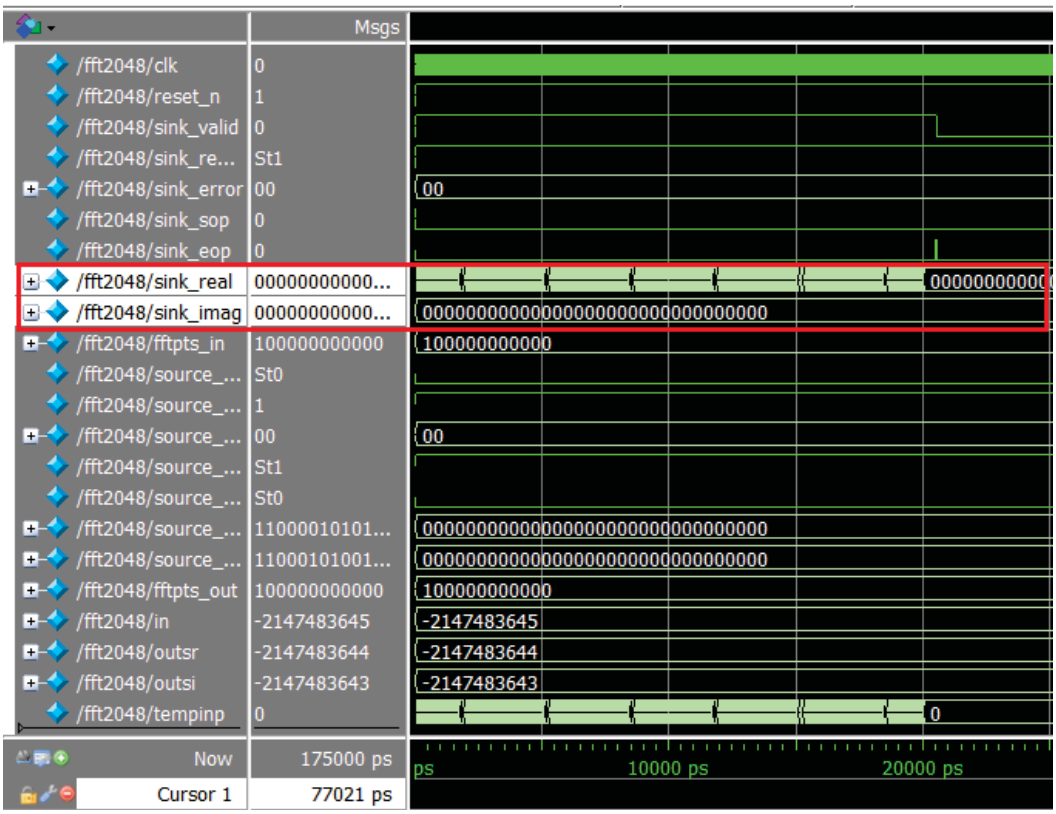

Figure 17 Signal C Inputs Being Processed

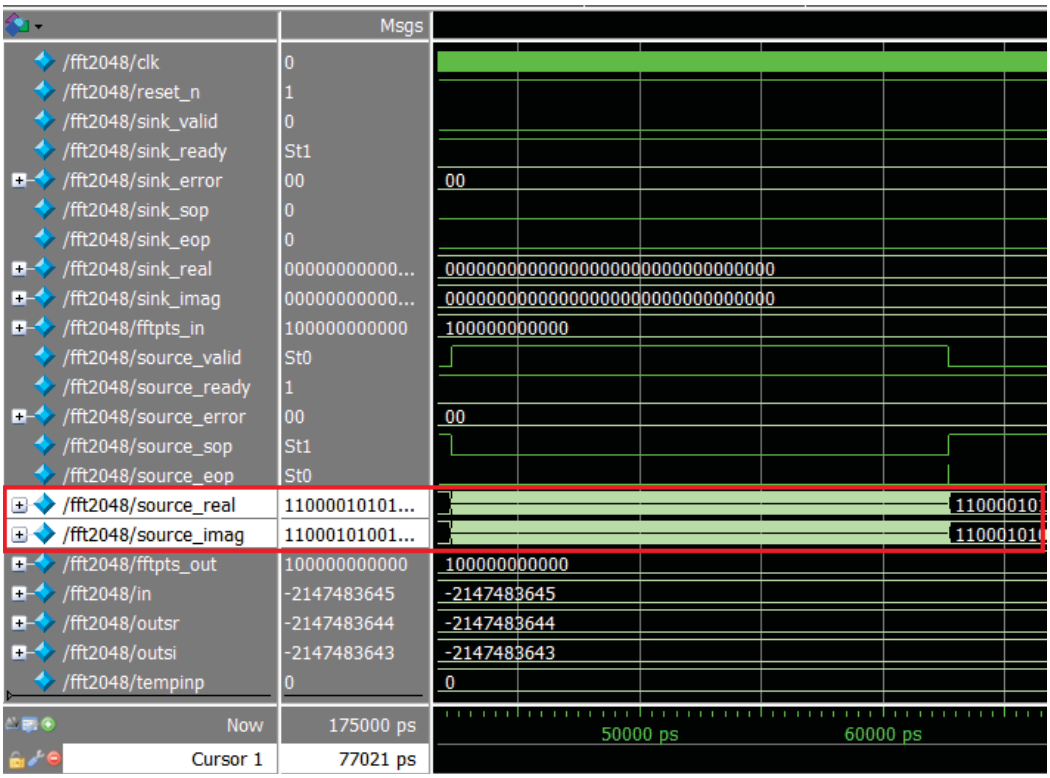

Figure 18 Signal C Outputs

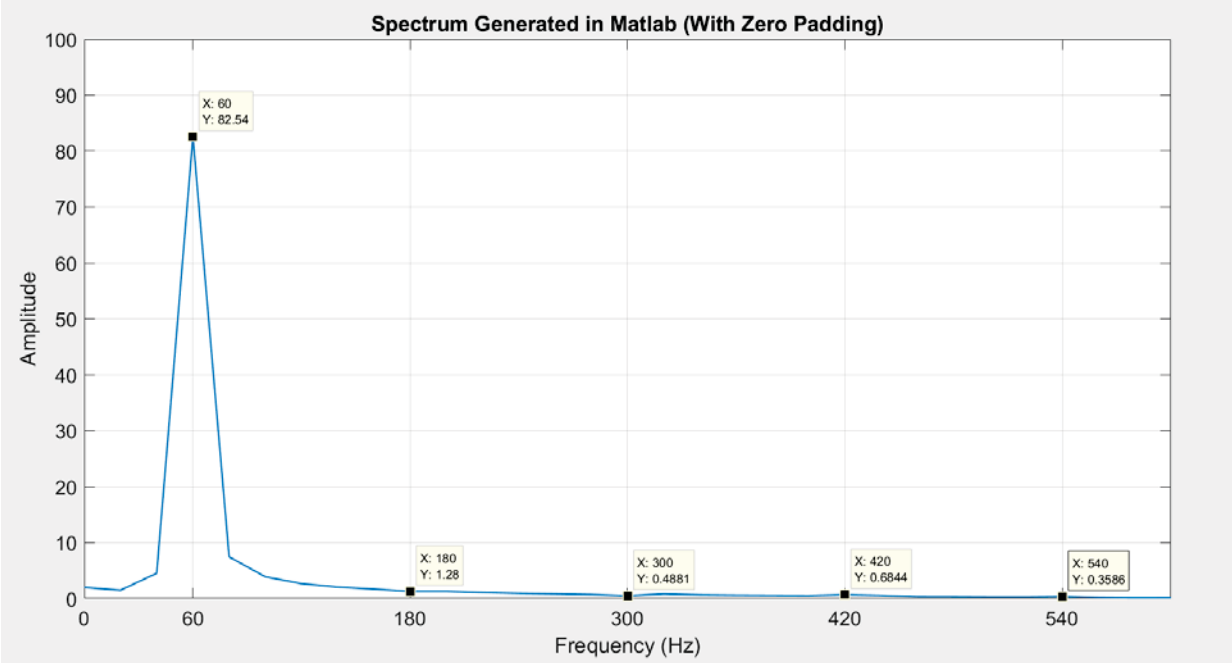

Figure 19 FFT Spectrum for Signal C Generated in MATLAB (With Zero Padding)

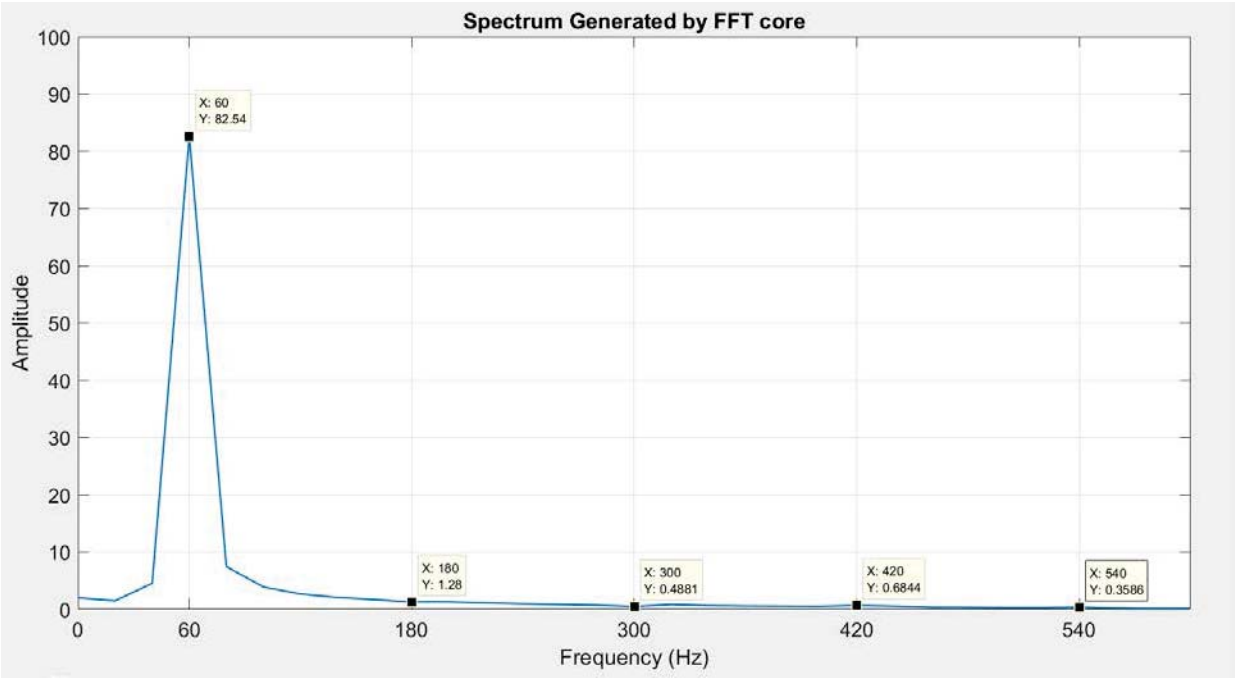

Figure 20 FFT Spectrum for signal C Generated by FFT IP Core System

Figures 17 and 18 show signal C being processed. Figure 17 shows the 2048 Inputs and figure 18 shows the 2048 outputs in their values, real and imaginary. Processing the inputs takes around 20505 pico-seconds (ps), and delivering the outputs takes around 42200 ps. Therefore, the whole process timing is about 62715 ps. Results are graphed and compared to the MATLAB results.

Figure 19 and Figure 20 compare the frequency domain graphs for signal C of MATLAB and the IP core system after performing zero padding. It is observed that the graphs are the same, which assures that the IP core system is functioning correctly.

Comparing the padded signal C with unpadded signal C, it is noticed that there is a small difference in the amplitude for the fundamental harmonic (60Hz). It is also noticed that the graph takes a minor curve between 60Hz and 180Hz in the padded, which also results in a change of the amplitude for third harmonics (180Hz). These changes between the two graphs are due to the zero padding. However, these changes are minor and expected, as zero padding is meant to improve the frequency resolution, which will slightly change the graph.

After comparing the results of all three signals between the theoretical values and the actual values, it can be observed that the theoretical values match the actual values, and the proposed system is ultimately working as it is designed to. The proposed system is a hardware, which means that it can be put on a chip or a device to analyze or test the harmonics distortion in power systems in real-time.

Chapter 5 - Conclusion and Future Research

5.1 Summary and Closing Remarks

In this thesis, the development of a real-time harmonic analyzer with digital hardware was discussed. The main reason behind this research was to prove that harmonic distortion can be detected and analyzed in real-time. Harmonic distortion in a power system usually does not have a constant value, therefore, detecting that value in real-time would positively improve the decision made to resolve this issue. To conduct this study, two signals we artificially constructed and one signal was recorded. A system was built using Altera software to analyze these signals and compare their results to the theoretical results from using MATLAB. The three signals A, B and C, were created to simulate real-life scenarios. These signals were processed and analyzed through the proposed system, and results matched the theoretical results, which highlighted the reason behind this research.

The developed system can be applied is many real-life applications. It can be implemented in residential, commercial, and industrial industries. The System can be used in applications such as hand-held power quality monitoring devices, substations monitoring systems, motor control centers, and many others. Some applications will require a higher number of data-points than others. Therefore, the number of data-points can easily be adjusted to fit for different applications. Other parameters can also be adjusted such as the transform direction, input order, and the output order.

5.2 Future Work and Recommendations

In this research, the system was designed and simulated as a proof of concept. Therefore, for future work, the system can be improved and developed to fit desired application. Some of these techniques are as follows:

- Build the hardware that would detect the signals and analyze them by displaying the results on a small LED screen.
- Add an analog-to-digital converter (ADC) to the system so it can analyze the signal directly without having to record it first.
- Expand the system with multiple FFT IP-cores in parallel that can analyze multiple signals at the same time.
- Develop the system to have an algorithm that will decide what actions need to be taken to improve the power factor depending on the THD level readings.
- Add an alarm to the system that would send a signal when a large harmonic component was detected in a device that would start a potential fire due to harmonic distortion.

Another way to improve the system would be to a history log to track the harmonic distortion value in a system and the time when that value was taken for long term analysis. Various other ways can be used to improve the system, though they are all a dependent on the desired application.

Bibliography

[1] B. Bose, “Power electronics and motion control-technology status and recent trends,” *PESC `92 Record. 23rd Annual IEEE Power Electronics Specialists Conference*.

[2] T. Gruzs, “A survey of neutral currents in three-phase computer power systems,” *Conference Record. Industrial and Commercial Power Systems Technical Conference*.

[3] M. Gibbon, “Energy Flow and Power Factor in Nonsinusoidal Circuits,” *Electronics and Power*, vol. 26, no. 3, p. 263, 1980.

[4] S. R. and D. D., "A Review of Harmonics Detection and Measurement in Power System", International Journal of Computer Applications, vol. 143, no. 10, pp. 42-45, 2016

[5] "Harmonics Detection and Filtering, Low Voltage Expert Guides", Schneider Electric, Technical leaflet, DBTP152GUI_EN, Retrieved from http://www.schneider-electric.com/en/download/document/DBTP152GUI_EN/

[6] Soni, Manish Kumar, and Nisheet Soni. "Review of causes and effect of harmonics on power system." *International Journal of Science, Engineering and Technology Research* 3.2 (2014): 214-220.Vol 3, Issue 2.

[7] Y. Ma, H. Yuan and X. Zhou, "Review of Harmonic Detection Methods for Active Power Filters", Advanced Materials Research, vol. 749, pp. 622-625, 2013.

[8] M. Karimi-Ghartemani and M. Iravani, "Measurement of Harmonics/Inter-harmonics of Time-Varying Frequencies", IEEE Transactions on Power Delivery, vol. 20, no. 1, pp. 23-31, 2005.

[9] D. McNamara, A. Ziarani and T. Ortmeyer, "A New Technique of Measurement of Nonstationary Harmonics", IEEE Transactions on Power Delivery, vol. 22, no. 1, pp. 387-395, 2007.

[10] F. Vatansever and A. Ozdemir, "A new approach for measuring RMS value and phase angle of fundamental harmonic based on Wavelet Packet Transform", Electric Power Systems Research, vol. 78, no. 1, pp. 74-79, 2008.

[11] G. W. Chang and C.-I. Chen, "Measurement techniques for stationary and time-varying harmonics," *IEEE PES General Meeting*, 2010.

[12] H. C. Lin, "Power Harmonics and Interharmonics Measurement Using Recursive Group-Harmonic Power Minimizing Algorithm," *IEEE Transactions on Industrial Electronics*, vol. 59, no. 2, pp. 1184–1193, 2012.

[13] Jaipreet Kaur Bhatti, Deepak Asati, (June 2012), Harmonic Detection using Microcontroller, International Journal of Computer Technology and Electronics Engineering (IJCTEE) Volume 2, Issue 3.

[14] Y. F. Wang and Y. W. Li, "An overview of grid fundamental and harmonic components detection techniques," *2013 IEEE Energy Conversion Congress and Exposition*, 2013.

[15] Z. Chu, M. Ding, S. Du, and X. Dong, "Normalized estimation of fundamental frequency and measurement of harmonics/interharmonics," *Journal of Control Theory and Applications*, vol. 11, no. 1, pp. 10–17, Oct. 2013.

[16] Jeena Joy, Amalraj P.M., Aswin Raghunath, Nidheesh M.N Vinu Joseph,(August 2014), Harmonic Analysis of 230 V AC Power Supply Using LPC2138 Microcontroller, Transactions on Engineering and Sciences ,Vol.2, Issue 8.

[17] F. Guihong, Z. Jing, Z. Yisong, Y. Yong, and Z. Bingyi, "Harmonic power detection and measurement device based on harmonic power flow analysis," *2005 International Conference on Electrical Machines and Systems*, 2005.

[18] M. Gibbon, "Energy Flow and Power Factor in Nonsinusoidal Circuits," *Electronics and Power*, vol. 26, no. 3, p. 263, 1980]

[19] J. Mazumdar, "SYSTEM AND METHOD FOR DETERMINING HARMONIC CONTRIBUTIONS FROM NONLINEAR LOADS IN POWER SYSTEMS," 2006.

[20] N. Mohan, T. M. Undeland, and W. P. Robbins, *Power electronics: converters, applications, and design*. New Delhi, India: Wiley India, 2008.

[21] M. H. Rashid, *Power electronics: circuits, devices, and applications*. New Delhi: Prentice Hall of India, 2006..

[22] A. Mceachern, W. Grady, W. Moncrief, G. Heydt, and M. Mcgranaghan, "Revenue and harmonics: an evaluation of some proposed rate structures," *IEEE Transactions on Power Delivery*, vol. 10, no. 1, pp. 474–482, 1995.

[23] "MATLAB," *Wikipedia*, 31-May-2017. [Online]. Available: https://en.wikipedia.org/wiki/MATLAB. [Accessed: 01-Jun-2017].

[24] Steve Hollasch / Last update 2015–Dec–2, "IEEE Standard 754Floating Point Numbers," *IEEE Standard 754 Floating-Point*. [Online]. Available: http://steve.hollasch.net/cgindex/coding/ieeefloat.html. [Accessed: 01-Jun-2017].

[25] J. G. Proakis, *DIGITAL SIGNAL PROCESSING USING MATLAB*. Florence, KY: Cengage Learning, Inc, 2012.

[26] S. He and M. Torkelson, "A new approach to pipeline FFT processor," *Proceedings of International Conference on Parallel Processing*, Honolulu, HI, 1996, pp. 766-770.1996